Current Clinical Microbiology Reports (2021) 8:68–86
https://doi.org/10.1007/s40588-021-00163-x

PARASITOLOGY (M BELEN CASSERA, SECTION EDITOR)

Naturally Occurring Alkaloids, Derivatives, and Semi-synthetic Modifications as Lead Compounds for the Development of New Anti-*Trypanosoma cruzi* Agents

Lucía Raquel Fernández[1,2] · Daniel Musikant[3] · Martin M. Edreira[3,4,5]

Accepted: 18 February 2021 / Published online: 4 March 2021

Abstract

Purpose of Review Despite recent advances, Chagas disease is still a public health issue that requires more efforts in order to develop efficient and safe drugs. Plants and fungi are the main source for semi-synthetic natural-inspired new molecules to treat human illness. In the present work, we summarize the main findings of natural-derived and semi-synthetic alkaloids against *Trypanosoma cruzi*.

Recent Findings Over the last 10 years, at least seven alkaloids groups with structural modifications, including 130 molecules and almost 100 semi-synthetic compounds derived from natural alkaloids, including hybrids molecules, modifications of aliphatic chain extension, chemical groups, and heteroatoms, were analyzed for its toxicity over parasites and mammalian cells.

Summary According to the available data, there are a good number of promising natural and/or semi-synthetic alkaloids that would meet the criteria to become candidates in the drug discovery process against *Trypanosoma cruzi* parasites. Main scaffolds that deserve special attention are natural quinolones, isoquinolines, and semi-synthetic hybrids molecules.

Keywords Alkaloids · *Trypanosoma cruzi* · Synthetic modifications · Antiparasitic activity

Introduction

In the twenty-first century, 604 drugs have been approved by the FDA, of which only seven were for the treatment of parasitic diseases [1]. In the specific case of Chagas disease, an important step forward was accomplished when a partnership between the Drugs for Neglected Diseases Initiative (DNDi) and private laboratories promoted the elaboration of a pediatric formulation of benznidazole (BZN). Some new drugs have been recently evaluated in clinical trials. Fexinidazole, a recently approved 5-nitroimidazole derivative, also developed by the DNDi in collaboration with Sanofi for the oral treatment of human African trypanosomiasis, is being tested against Chagas disease [2] and results of the Phase II proof-of-concept study were expected in 2020 [3]. Additionally, separate clinical trials with azoles, posaconazole and E1224, recently

Lucía Raquel Fernández and Daniel Musikant contributed equally to this work.

This article is part of the Topical Collection on *Parasitology*

✉ Martin M. Edreira
mme2@pitt.edu

Lucía Raquel Fernández
lfernandez@conicet.gov.ar

Daniel Musikant
musi90@gmail.com

[1] Departamento de Química Orgánica, Facultad de Ciencias Exactas y Naturales, Universidad de Buenos Aires, Buenos Aires, Argentina

[2] CONICET-Universidad de Buenos Aires, Unidad de Microanálisis y Métodos Físicos Aplicados a la Química Orgánica (UMYMFOR), Buenos Aires, Argentina

[3] Departamento de Química Biológica, Facultad de Ciencias Exactas y Naturales, Universidad de Buenos Aires, Buenos Aires, Argentina

[4] Instituto de Química Biológica de la Facultad de Ciencias Exactas y Naturales (IQUIBICEN), CONICET-Universidad de Buenos Aires, 1428 Buenos Aires, Argentina

[5] Department of Pharmacology and Chemical Biology, School of Medicine, University of Pittsburgh, Pittsburgh, PA, USA

ended. Unfortunately, in addition to some safety issues with E1224 at the highest dose [4], results showed that at the doses used for the management of invasive fungal infections, these compounds were significantly less effective to induce sustained parasitemia suppression 1 year after treatment initiation than BZN at the conventional dose (2.5 mg/kg twice a day for 60 days) [5••]. Still, no new chemical entities have been approved to replace the old drugs (i.e., BZN and nifurtimox (NFT)) currently used against *Trypanosoma cruzi*, the etiological agent of Chagas disease, which have shown to be highly toxic and not effective, especially during the chronic stage of the disease.

New scaffolds with the potential to enter the drug discovery process for Chagas disease are urgently needed. In this regard, it is a well-known fact that natural products comprise thousands of compounds with enormous structural diversity and biological activities. Either harnessed directly by isolation from the natural source, with semi-synthetic structural modifications or employed to inspire new compounds, natural products have participated, and still actively participate, in the chemical space of drugs approved to treat human conditions.

In particular, structural richness of alkaloids is reflected in their chemical, biological, and pharmacological properties. Their historical role in the drug discovery process and eventual arrival at a medicinal formulation can be summarized with the two most famous examples: morphine, approved as an analgesic by the FDA in 1827, and the antimalarial quinine, approved in 1950. In addition to quinine, other *Cinchona* alkaloids including quinidine, cinchonine, and cinchonidine all shown to be effective against malaria [6]. More recently, tafenoquine, an 8-aminoquinoline that share the quinoline core of quinine, has been approved for malaria prophylaxis and treatment [7], showing that quinoline derivatives could still be exploited in order to find new antichagasic agents.

When targeting the parasite, it is important to consider that *T. cruzi* has a complex life cycle, involving four developmental stages between the insect vector and the mammalian host. Metacyclic trypomastigotes, present in the intestinal lumen of the insect vector, gain access to the mammalian host through feces contamination at the site of the insect bite wound. As an intracellular parasite in the mammalian host, they infect cells close to the site of entry, where they differentiate into the proliferative amastigote form. After several rounds of replication, amastigotes differentiate to trypomastigotes that are released into the bloodstream, from where they disseminate by infecting distant tissues, or are taken up by the insect vector during a bloodmeal [8]. In addition to a complex life cycle, the parasite presents multiple strains with a high degree of genetic variability. *T. cruzi* genetic diversity has been classified into six Discrete Typing Units (DTUs): the ancestral strains DTU-I and II, homozygote-derived hybrids DTU-III and IV, and heterozygote hybrids DTU-V and VI [9]. Interestingly, as a consequence of this variability, in vitro and in vivo differential drug susceptibility among strains has been reported [10–12].

In this review, the most promising alkaloids were classified according to their main structure and origin, activity against different stages of *T. cruzi* and modifications, and were discussed.

Aporphines

Dicentrinone (**1**) (Fig. 1), an oxoaporphine alkaloid isolated from fresh leaves of *Ocotea puberula* (Lauraceae), showed a half-maximal inhibitory concentration (IC_{50}) value of 16.4 ± 1.7 μM against free trypomastigotes of the Y strain of *T. cruzi*. This value was comparable to that of BZN (18.7 ± 4.1 μM). No cytotoxic effect was observed on NCTC cells at the highest concentration tested. The resulting selectivity index (SI) was > 12.2 [13]. This compound was also isolated from subterranean stem bark of *Duguetia furfuracea* (Annonaceae) along with four other aporphine alkaloids: duguetine (**2**), duguetine β-N-oxide (**3**), N-methyl-tetrahydropalmatine (**4**), and N-methylglaucine (**5**) (Fig. 1) [14]. While compounds **4** and **5** were inactive, duguetine (**2**) showed an IC_{50} of 9.32 μM and was the most active of these structures; however, compound **3** that only differs in the oxidation of the amino group was 3 times less active (IC_{50}: 30.79 μM). Both compounds presented low 50% cytotoxic concentration (CC_{50}) against three tumor cell lines, not exceeding 12 μM in any of the three cases [14]. Extraction from branches of another Annonaceae, *Annona foetida*, led to the isolation of liriodenine (**6**) and *O*-methylmoschatoline (**7**) (Fig. 1). The IC_{50} values for these compounds were above 100 μM against the epimastigote form, and moderate activity was observed against the trypomastigote form (14.5 ± 0.07 and 11.83 ± 5.60 μM, respectively) [15].

Naphthylisoquinolines

There are a great number of reports about naphthylisoquinoline alkaloids with antiparasitic activity, the majority being isolated from lianas from the *Ancistrocladus* genus [16]. The C–C bond between the naphtyl and isoquinoline core is sometimes sterically hindered for rotation, generating atropoisomers. This depends on the position of the union between the two moieties. Thus, two possible configurations along the coupling axis, named *P* or *M* based on the molecule's helicity, are observed. Also, different degrees of methylation can be found and the isoquinoline core can bear one or two asymmetric carbons. As a consequence, the structural diversity of naphthylisoquinolines is enormous.

The C-5,C-8′ coupling is highly occurrent, and of the nine *P*-configured compounds (**8**–**16**, Fig. 2) whose anti-*T. cruzi* activity has been evaluated, the most active was ancistroealaine A (**8**) [17]. This fully methylated structure

Fig. 1 Structures of aporphines **1**–**7**

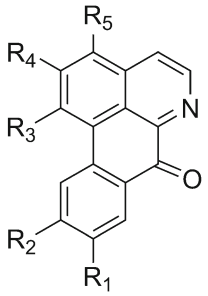

(1) Dicentrinone R_1=R_2=OCH_3; R_3=R_4=OCH_2O; R_5=H
(6) Liriodenine R_1=R_2=R_5=H; R_3=R_4=OCH_2O
(7) O-methylmoschatoline R_1=R_2=H; R_3=R_4=R_5=OCH_3

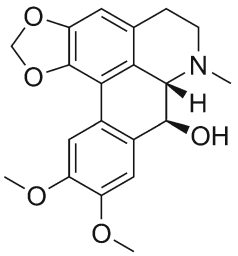

(2) Duguetine

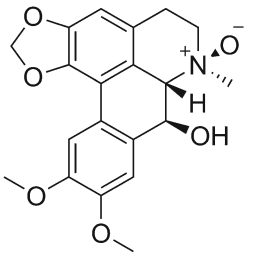

(3) Duguetine-β-N-oxide

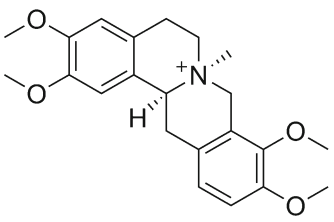

(4) N-methyl-tetrahydropalmatine

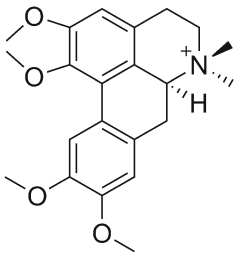

(5) N-methylglaucine

possesses a C–N double bond and *S* configuration at C-3 of the isoquinoline residue. All compounds were tested against trypomastigotes (Tulahuen C4, stably expressing β-galactosidase (β-gal) co-incubated with L6 cells, and the cytotoxic effect on these cell lines was also evaluated. The IC_{50} value for ancistroealaine A (**8**) was 5.6 μM with no cytotoxicity (CC_{50} > 214 μM, SI > 38), followed by 6,5′-O,O-didemethylancistroealaine A (**9**) with an IC_{50} of 16.3 μM and still no cytotoxic effect (CC_{50} > 230 μM) [18]. The replacement of methoxy groups at positions C-6 and C-5′ by

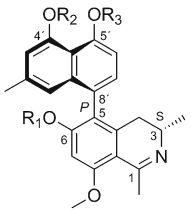

(8) Ancistroealaine A R_1=R_2=R_3=CH_3
(9) 6,5′-O,O-didemethylancistroealaine A R_1=H; R_2=CH_3; R_3=H
(10) 6-O-demethylancistroealaine A R_1=H; R_2=R_3=CH_3
(11) Ancistrolikokine D R_1=R_2=H; R_3=CH_3

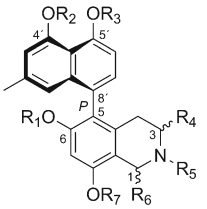

(12) Korupensamine A R_1=H; R_2=CH_3; R_3=H; R_4=(R)β–CH_3; R_5=H; R_6=(R)α–CH_3; R_7=H
(13) Ancistrocongoline A R_1=H; R_2=CH_3; R_3=H; R_4= (R)β–CH_3; R_5=CH_3; R_6=(R)α–CH_3; R_7=H
(14) Ancistrocongoline B R_1=R_2=R_3=CH_3; R_4= (R)β–CH_3; R_5=CH_3; R_6=(R)α–CH_3; R_7=H
(15) Ancistroealaine B R_1=R_2=CH_3; R_3=CH_3; R_4= (S)α–CH_3; R_5=H; R_6=(S)β–CH_3; R_7=CH_3
(16) Ikelacongoline A R_1=H; R_2=R_3=CH_3; R_4= (R)β–CH_3; R_5=CH_3; R_6=(R)α–CH_3; R_7=H

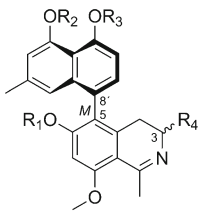

(17) Ancistrotanzanine B R_1=R_2=R_3=CH_3; R_4=(S)α-CH_3
(18) Ancistectorine D R_1=CH_3; R_2=H; R_3=CH_3; R_4=(S)α-CH_3
(19) Ancistrobonsoline A_1 R_1=H; R_2=CH_3; R_3=H; R_4=(R)β-CH_3
(20) Ancistrobonsoline A_2 R_1=R_2=CH_3; R_3=H; R_4=(R)β-CH_3

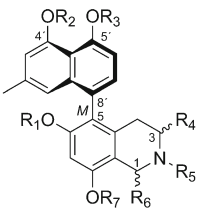

(21) Ancistrotectoriline A R_1=R_2=R_3=CH_3; R_4=(S)α–CH_3; R_5=H; R_6=(S)β–CH_3; R_7=CH_3
(22) 5-epi-4′-O-demethylancistrobertsonine C R_1=CH_3; R_2=H; R_3=CH_3; R_4=(S)α–CH_3; R_5=CH_3; R_6=(R)α–CH_3; R_7=CH_3
(23) 5-epi-6-O-methylancistrobertsonine A R_1=R_2=R_3=CH_3; (S)α–CH_3; R_5=CH_3; R_6=(S)β–CH_3; R_7=CH_3
(24) Ancistrocongoline C R_1=H; R_2=R_3=CH_3; R_4=(R)β–CH_3; R_5=CH_3; R_6=(R)α–CH_3; R_7=CH_3
(25) Ancistrobrevine B R_1=H; R_2=CH_3; R_3=CH_3; R_4=(S)α–CH_3; R_5=H; R_6=(S)β–CH_3; R_7=CH_3
(26) 5′-O-demethylancistrobrevine B R_1=H; R_2=CH_3; R_3=H; R_4=(S)α–CH_3; R_5=H; R_6=(S)β–CH_3; R_7=CH_3
(27) Ikelacongoline B R_1=H; R_2=R_3=CH_3; R_4=(R)β–CH_3; R_5=CH_3; R_6=(R)α–CH_3; R_7=H
(28) Ikelacongoline C R_1=H; R_2=R_3=CH_3; R_4=(R)β–CH_3; R_5=CH_3; R_6=(S)β–CH_3; R_7=CH_3

Fig. 2 Structures of naphthylisoquinolines **8**–**28**

hydroxyl groups reduced the antiparasitic activity; however, O-methylation of C-6 was more important as it could be observed for 6-O-demethylancistroealaine A (**10**) (IC_{50}: 25.9 μM, CC_{50} > 100 μM) where the activity was not restored by the O-methylation of C-5′ [18]. Ancistrolikokine D (**11**), with hydroxyl groups at C-4 and C-6, was even less active than the already mentioned compounds (IC_{50}: 32.6 μM) [19]. The remaining five *P*-configured, C-5,C-8′-coupled naphthylisoquinolines (**12**–**16**) were non-cytotoxic but also not active against *T. cruzi* (the lowest IC_{50} is 38.2 μM for korupensamine A (**12**)) [20, 21]. Structurally, compounds **12** to **16** lacked the C–N double bond resulting in one more stereocenter at C-1, and none of those was fully methylated.

Twelve *M*-configured C-5,C-8′-coupled isomers were evaluated against β-gal Tulahuen trypomastigotes (Fig. 2). The *M*-configured isomer of ancistroealaine A (**8**), ancistrotanzanine B (**17**), was the most active of this series with an IC_{50} of 3.58 μM, but the CC_{50} value was 19.33 μM [22]. The demethylation of C-4′ had little effect on the activity against *T. cruzi* or cytotoxicity as it could be observed by the values of these parameters obtained for ancistectorine D (**18**) (IC_{50} 4.439 μM and CC_{50} 11.34 μM) [23]. Ancistrobonsoline A_1 (**19**) and A_2 (**20**), where the configuration at C-3 changes from *S* to *R*, were inactive and weakly cytotoxic (IC_{50} 109.3 and 80.1 μM and CC_{50} 114 and 52.8 μM, respectively) [24]. Changes involving the conversion of the C–N double bond to a single one and the generation of a new stereocenter provoked some loss of activity for ancistrotectoriline A (**21**) (IC_{50} 18.50 μM CC_{50} 14.5 μM) and 5-epi-4′-O-demethylancistrobertsonine C (**22**) (IC_{50} 11.1 μM CC_{50} > 100 μM). The rest of the compounds (**23**-**28**) were inactive [18, 20, 21, 24, 25].

Another frequent coupling arrangement for this type of alkaloids is C-5,C1′ (Fig. 3). In this case, O-mehtylancistrocladinine (**29**), the C-5,C-1′ regioisomer of ancistroealaine A (**8**), was inactive [26]. Only ancistrobenomine A (**30**) was moderately active with an IC_{50} of 11.45 μM, but moderately cytotoxic (CC_{50} 29.35 μM) as well [27]. Compounds **31**–**45** were inactive [18, 25–28]. These results could indicate that these particular coupling positions lead to compounds without antiparasitic activity.

The majority of the tested C-7,C-3′-coupled nahpthylisoquinoline alkaloids (Fig. 4) were *M*-configured. Ancistotectorine (**46**) showed an IC_{50} of 10.2 μM and CC_{50} of 47.2 μM (SI: 4.71) [26]. Once again, a loss of activity was observed by demethylation of C-6, as for ancistrotanzanine C (**47**) (IC_{50}: 34.35 μM, CC_{50}: 47.2 μM). Dioncophylline E (**48**) was not oxygenated at the C-6 position; thus, a slow conversion from the *P* to *M* configuration was possible. Compounds **48**-**50** were moderately active or inactive [26, 29, 30].

Compounds with C-7,C-1′ or C-7,C-8′ have been inactive so far [20, 23, 25, 31–33]. Ancistrotanzanine A (**51**), a C-5,C-3′-coupled naphthylisoquinoline alkaloid, showed good activity (IC_{50} 4.20 μM) and moderate cytotoxicity (CC_{50} 19.33 μM) [22]. Three N,C-8′-coupled naphthylisoquinoline alkaloids, ancistrocladinium A (**52**), 4′-O-demethylancistrocladinium A (**53**), and 6,4′-O-didemethylancistrocladinium A (**54**) were evaluated against Tulahuen C4 trypomastigotes of *T. cruzi* [34]. In this case, the fully methylated structure (**52**) was inactive (IC_{50} > 70 μM); however, demethylation of position C-6 did provoke a loss of activity as observed by the IC_{50} values of compounds **53** and **54**. Compound **53** bears a phenolic group at C-4′ and had the best activity with an IC_{50} of 0.03 μM (CC_{50}: 53.9 μM, SI:1,796), but for compound **54**, with phenolic groups at C-4′ and C-6, the IC_{50} increased to 6.0 μM, which is still a significant activity, but with a SI of 11.52 (CC_{50} 69.1 μM). Dimeric naphthylisoquinoline alkaloids have also been isolated but the activities reported so far are moderate for this type of structures, except for mbandakamine B_2 (**55**) that showed an IC_{50} of 2.98 μM but a very high cytotoxicity as well (CC_{50}: 1.37 μM) [21, 31, 35–38]. The structures of compounds **51**-**55** are shown in Fig. 4.

Furoquinolines

There are few reports on the antiprotozoal activity of this type of alkaloids in the last 10 years. Costa et al. reported that γ-fagarine (**56**) displayed weak activity against epimastigotes of the Y strain (IC_{50}: 33.4 ± 1.2 μM; Bz IC_{50}: 20 μM) [39]. Previous reports informed that the widely distributed skimmianine (**57**), kokusaginine (**58**), masculine (**59**), and flindersiamine (**60**) were inactive [40, 41] (Fig. 4).

Quinolinones

Twelve quinolinic alkaloids, waltheriones A, C, E-L, antidesmone, and 8-deoxoantidesmone (**61**–**72**, Fig. 5) were isolated from the aerial parts and roots of *Waltheria indica* [42, 43]. The compounds were evaluated against trypomastigotes (Tuluhaen C2C4 (LacZ)) in L6 cells as host. Except for waltherione A (**61**), which showed low activity, the rest of the compounds displayed potent activity against amastigotes (Tuluhaen C2C4 (LacZ)) with IC_{50} in the submicromolar range. However, cytotoxicity against L6 cells was also high for most of the alkaloids. Waltherione G (**65**) presented the lowest IC_{50} value (0.02 μM), and a CC_{50} of 0.64 μM resulting in a good SI 33.8. Waltheriones H (**66**) and K (**69**) both showed IC_{50} of 0.04 μM but poor selectivity (SI 6.5 and 1.8, respectively). Antidesmone (**71**) showed the highest SI (595). For this compound, the IC_{50} and CC_{50} values were 0.062 μM and 36.93 μM, respectively [43, 44]. Waltherione C (**62**) also showed good activity (IC_{50}: 1.93 μM) and low cytotoxicity (CC_{50}: 101.23 μM).

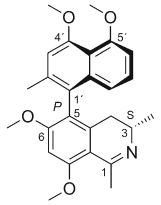

(29) O-methylancistrocladinine

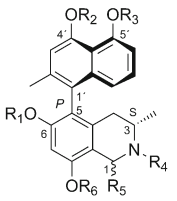

(31) O,N-dimethylancistrocladine R_1=R_2=R_3=R_4=CH_3; R_5=(S)β–CH_3; R_6=CH_3
(32) 5′-O-demehtylancistrocline R_1=H; R_2=CH_3; R_3=H; R_4=CH_3; R_5=(R)α–CH_3; R_6=CH_3
(33) Ancistrocoline R_1=H; R_2=R_3=R_4=CH_3; R_5=(R)α–CH_3; R_6=CH_3
(34) Ancistrobrevine E R_1=H; R_2=R_3=CH_3; R_4=H; R_5=(S)β–CH_3; R_6=H
(35) Ancistrobrevine F R_1=R_2=H; R_3=CH_3; R_4=H; R_5=(S)β–CH_3; R_6=H
(36) Ancistrobrevine G R_1=H; R_2=CH_3; R_3=R_4=H; R_5=(S)β–CH_3; R_6=H

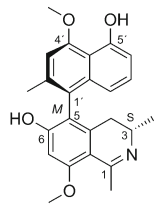

(37) 5′-O-demethylhamatinine

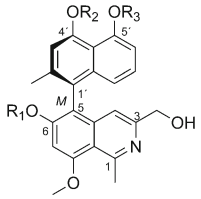

(30) Ancistrobenomine A R_1=CH_3; R_2=H; R_3=CH_3
(38) 6-O-demethylancistrobenomine A R_1=H; R_2=R_3=CH_3
(39) Ancistrobenomine B R_1=R_2=R_3=CH_3
(40) Ancistrobenomine C R_1=H; R_2=R_3=CH_3

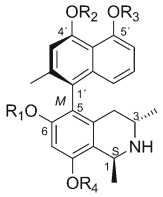

(41) 5′-O-demethylhamatine R_1=H; R_2=CH_3; R_3=H; R_4=CH_3
(42) 5-epi-ancistectorine A_2 R_1=R_2=R_3=CH_3; R_4=H
(43) 5-epi-ancistrobrevine E R_1=H; R_2=R_3=CH_3; R_4=H
(44) 5-epi-ancistrobrevine F R_1=R_2=H; R_3=CH_3; R_4=H
(45) 6-O-methylhamatine R_1=R_2=R_3=CH_3; R_4=CH_3

Fig. 3 Structures of naphthylisoquinolines **29**–**45**

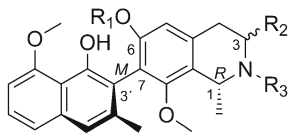

(46) Ancistrotectorine R_1=CH_3 R_2=(S)α–CH_3; R_3=CH_3
(47) Ancistrotanzanine C R_1=H; R_2=(S)α–CH_3; R_3=CH_3

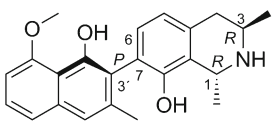

(48) Dioncophylline E

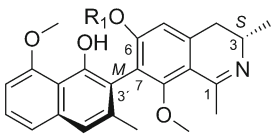

(49) Ancistrocladinine R_1=CH_3
(50) Ancistroheynine B R_1=H

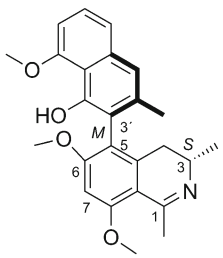

(51) Ancistrotanzanine A

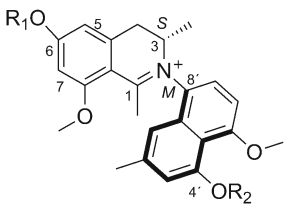

(52) Ancistrocladinium AR_1=R_2=CH_3
(53) 4′-O-demethylancistrocladinium A R_1=CH_3; R_2=H
(54) 6,4′-O-demethylancistrocladinium A R_1=R_2=H

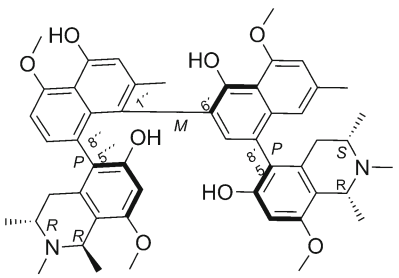

(55) Mbandakamine B_2

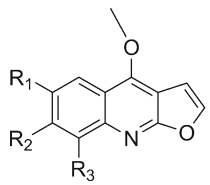

(56) γ-fagarine R_1=R_2=H; R_3=OCH_3
(57) Skimmianine R_1=H; R_2=R_3=OCH_3
(58) Kokusaginine R_1=R_2=OCH_3; R_3=H
(59) Maculine R_1=R_2=OCH_2O; R_3=H
(60) Flindersiamine R_1=R_2=OCH_2O; R_3=OCH_3

Fig. 4 Structures of compounds **46**–**60**

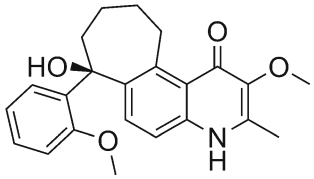

(61) Waltherione A

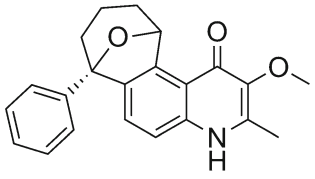

(62) Waltherione C

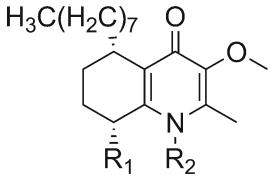

(63) Waltherione E R_1=OCH_3; R_2=H
(68) Waltherione J R_1=H; R_2=OCH_3
(69) Waltherione K R_1=R_2=OCH_3
(71) Antidesmone R_1= =O; R_2=H

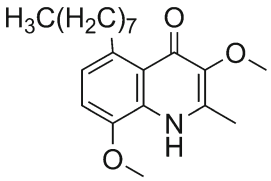

(64) Waltherione F

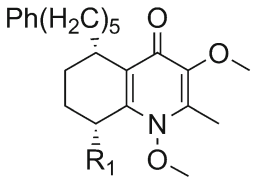

(65) Waltherione G R_1=H
(66) Waltherione H R_1=OCH_3

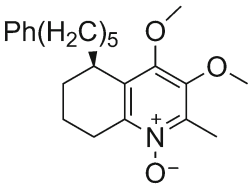

(70) Waltherione L

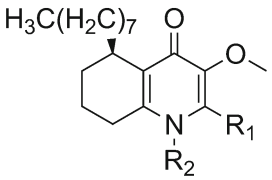

(67) Waltherione I R_1=CH_3; R_2=H
(72) 8-deoxoantidesmone R_1=CH_2OH; R_2= OCH_3

Fig. 5 Structure of compounds **61**–**72**

Indoles

Staurosporine (**73**), originally isolated from *Streptomyces staurosporeus*, is a potent non-selective inhibitor of protein kinases [45, 46]. Due to the fact that protein kinases are essential for parasite survival and pathogenicity, four staurosporines (**73**–**76**, Fig. 6) isolated from cultures of *Streptomyces sanyensis* PBLC04, the structurally related commercial indolocarbazoles alkaloids: K252a (**77**), K252b (**78**), K252c (**79**), a synthetic PKC inhibitor, arcyriaflavin A (**80**), and rebeccamycin (**81**), a DNA topoisomerase I inhibitor isolated from *Streptomyces aerocolonigenes*, were tested against epimastigotes of the Y strain of *T. cruzi*. Staurosporine (**73**) and 7-oxostaurosporine (**74**) were the most active compounds followed by the synthetic alkaloids **77** and **78** with IC_{50} 3.63 ± 0.77, 1.58 ± 0.52, 4.00 ± 0.24 and 7.41 ± 0.93 μM, respectively. It is worth noticing that **74** is twice as active than **73** and that the only difference between these two structures is a carbonyl group at C-7. Compounds **75** and **76** were moderately active (IC_{50} 17.10 ± 1.64 and 12.50 ± 2.06, respectively) while **79**–**81** were inactive. The cytotoxic effect of the compounds was performed on the J774A.1 macrophage cell line. CC_{50} values for **73** and **74** were 8.74 ± 0.72 and 5.20 ± 1.75 μM, respectively. The selectivity index in these cases was very low. Compounds **75** and **76** showed CC_{50} above 40 μM, although the selectivity index remained low [47] (Fig. 6).

Tryptophan-derived β-carboline alkaloids canthin-6-one (**82**), 5-methoxy-canthin-6-one (**83**), and canthin-6-one N-oxide (**84**) isolated from stem bark of *Zanthoxylum chiloperone* var. *angustifolium* (Fig. 7A) were evaluated on trypomastigotes of the Y strain. Compounds **82** and **83** induced 79 and 75% trypomastigotes lysis (Y strain) at 1.135 μM and 999 μM, respectively. Activity against amastigotes expressing β-galactosidase, for both compounds at 15.1 μM, was 90.0 and 66.4%, respectively. Cytotoxic effects were not observed at 15 μM on NCTC 929 cells for both compounds [48]. In vivo studies were performed using Balb/c mice for acute and chronic disease models of infection with CL *Trypanosoma cruzi*. For the acute model, BZN was administered to BALB/c mice orally at 50 mg/kg/day and canthin-6-one (**82**), 5-methoxy-canthin-6-one (**83**), and canthin-6-one N-oxide (**84**) were administered orally or subcutaneously at 5 mg/kg/day for 2 weeks. The mean parasitemia at day 28 for BZN and oral canthin-6-one-

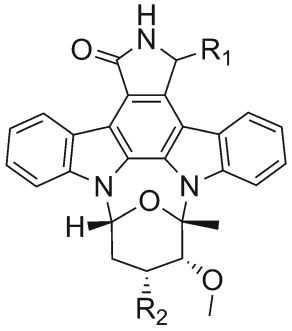

(73) Staurosporine R_1=H; R_2=$NHCH_3$
(74) 7-Oxostaurosporine R_1= =O; R_2=$NHCH_3$
(75) 4'-Demethylamine-4'-oxostaurosporine R_1=H; R_2= =O

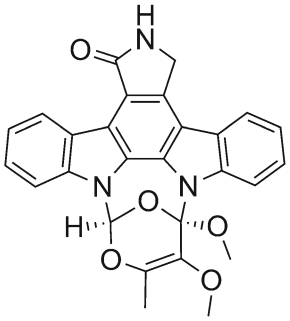

(76) Streptocarbazole B

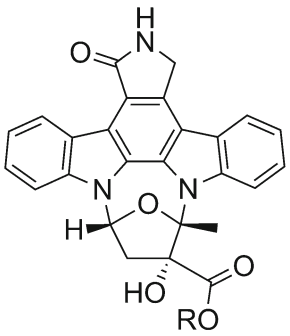

(77) K252a R=CH_3
(78) K252b R=H

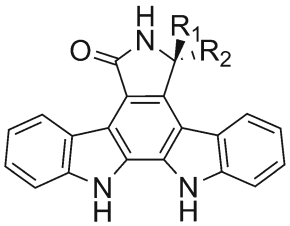

(79) K252c R_1=R_2=H
(80) Arcycriaflavin A R_1=R_2= =O

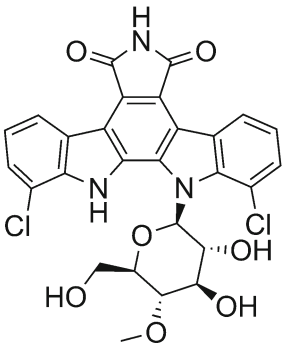

(81) Rebeccamycin

Fig. 6 Structures of compounds **73**–**81**

treated mice was significantly reduced (P = 0.0001 versus controls). Untreated mice presented 45% mortality whereas the group orally treated with compound **82** had a 100% survival rate. Absence of detectable parasitemia was observed for 19 out of 20 mice treated with canthin-6-one (**82**), 10% higher than with BZN.

The indolic alkaloid, violacein (**85**), and side-product deoxyviolacein (**86**) (Fig. 7A), produced in recombinant *E. coli* strains expressing the complete or partial synthetic violacein operon, inhibited Tulahuen trypomastigotes (DTU-VI) stably expressing β-galactosidase (β-gal) with an IC_{50} of 1.51 μM ± 0.4 and 50 μM, respectively. Although violacein displayed good activity, it was toxic against COS-7 and HepG2 cell lines (CC_{50} 2.5 μM and 1.4 μM, respectively). In contrast, deoxyviolacein showed low toxicity against mammalian cell lines [49•]. From these results, it is evident that the phenol group is important for both antiparasitic and cytotoxic activities.

Fractionation of the ethyl acetate extract of the marine bacterium *Bacillus pumilus* isolated from the black coral *Antipathes* sp. yielded three moderately active indolic alkaloids: 3-hydroxyacetylindole (**87**), N-acetyl-β-oxotryptamine (**88**), and 3-formylindole (**89**) (Fig. 7A). Compounds were evaluated on amastigotes (Tulahuen β-gal) and results showed IC_{50} values of 20.6, 19.4, and 26.9 μM, respectively. Cytotoxicity against Vero cells was moderate (IC_{50} values of 149, 66, and 87 μM, respectively) [50]. Given the structural similarities, the length and substitution of the side chain attached to carbon C-3 does not appear to produce a significant difference in the biological activity. The authors compared the activity of alkaloid **87** with that of tryptophol (**90**, Fig. 7A). This metabolite is produced by plants, bacteria, fungi, and sponges, and induces sleep in humans. Since the IC_{50} for this indolyl alcohol was 30.6 μM, the authors concluded that the presence of an electron-attracting group in the side chain, like the carbonyl at C-1′, enhanced the biological activity.

Two oxoindoles (91–92) and a plumerane-type alkaloid (**93**) (subtype haplophitine) (Fig. 8) were isolated from the aerial parts and roots of *Aspidosperma rigidum* (Apocynaceae) [51]. In the same work, two more compounds (**94**–**95**, Fig. 8) belonging to the same classification were extracted from the bark of *Aspidosperma schultesii.* Only caboxine B (**91**) displayed moderate activity (IC_{50} 26.60 μM) against epimastigotes (Y strain) with no toxicity against CHO cells (>100 μM). The rest of the compounds were

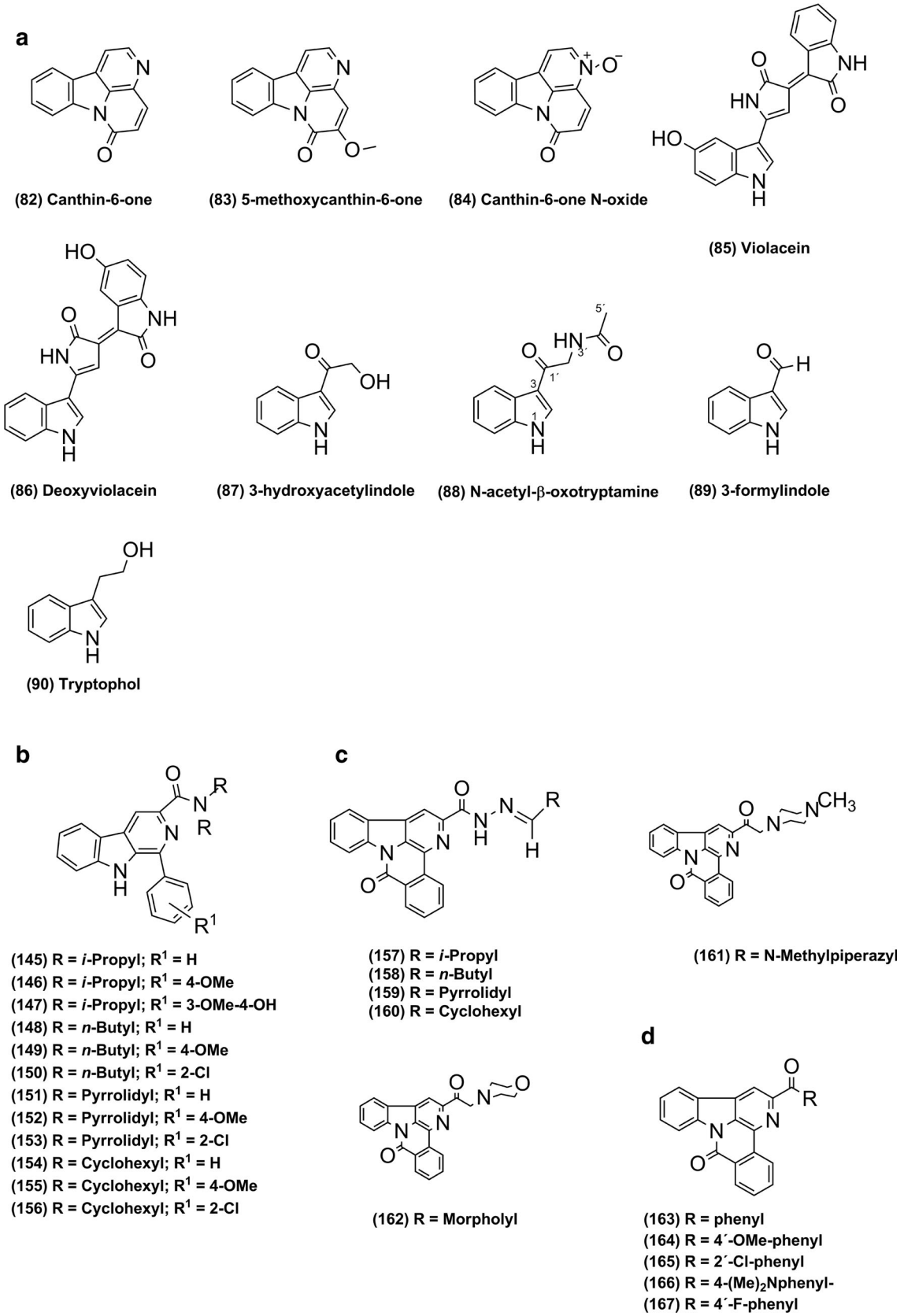

Fig. 7 Canthin-6-one derivatives. (A) Obtained from a natural source (**82**–**90**) or (B–D) obtained by synthesis. (B) 1-(substituted phenyl)-βcarbolines (**145**–**156**). (C) Methyl 6-Oxobenzo[4,5]canthine-2-carboxylate derivatives (**157**–**162**). (D) N-(substituted benzylidene)-carbohydrazide (**163**–**167**)

inactive. It is worth mentioning that the only difference between caboxine B (**91**) and carapanaubine (**92**) is a methoxy group and appears to affect the performance of each compound against *T. cruzi*. Compounds **96**–**102** (Fig. 8) were obtained from the leaves of another Apocynaceae, *Geissospermum reticulatum*, and were all inactive [52].

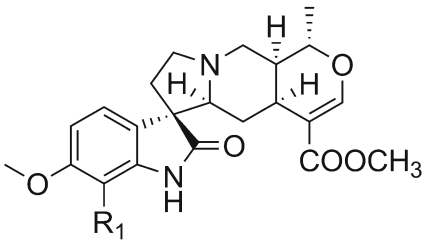

(91) Caboxine B R_1=H
(92) Carapanaubine R_1=OCH_3

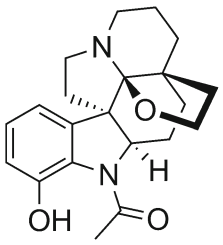

(93) Haplocidine

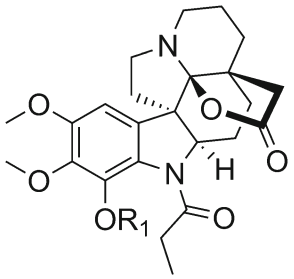

(94) 18-oxoaspidoalbine R_1=H
(95) 18-Oxo-O-methylaspidoalbine R_1=CH_3

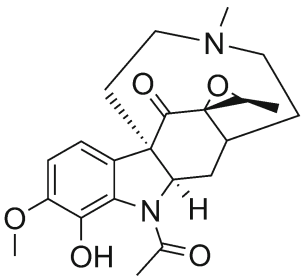

(96) 10-Demethoxy-12-hydroxy-17,19-epoxygeissovelline

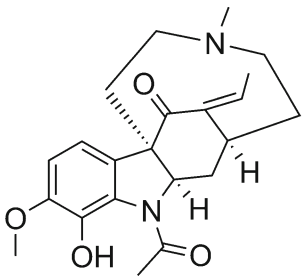

(97) (Z)-10-Demethoxy-12-hydroxygeissovelline

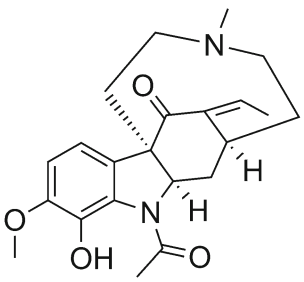

(98) (E)-10-Demethoxy-12-hydroxygeissovelline

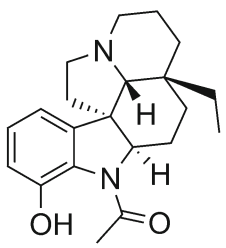

(99) O-Demethylaspidospermine

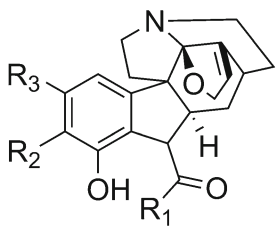

(100) Geissospermidine R_1=CH_3; R_2=R_3=H
(101) 10-Methoxygeissospermidine R_1=CH_3; R_2=H; R_3=OCH_3
(102) N-Deacetyl-N-butanoylgeissospermidine R_1=$CH_2CH_2CH_3$; R_2=R_3H

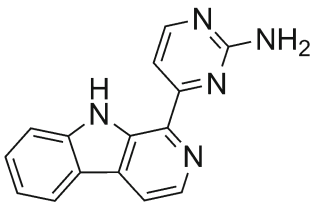

(103) Annomontine

Fig. 8 Structures of compounds **91**–**103**

A pyrimidine-β-carboline-type alkaloid, annomontine (**103**) (Fig. 8), isolated from the branches of *Annona foetida* was evaluated on epimastigotes and trypomastigotes (Y strain). The compound was inactive against the proliferative form (epimastigotes) and moderate active against the infective one (trypomastigotes) (IC_{50} = 16.08 ± 7.28 μM) [15]

Amaryllidaceae Alkaloids

Lycorine (**104**), hippeastrine (**105**), crinine (**106**), haemanthamine (**107**), narciclasine (**108**), tazettine (**109**), montanine (**110**), sanguinine (**111**), and 1-O-acetylcaranine (**112**) alkaloids were isolated from extracts of different *Narcissus* species (Fig. 9) [53]. These compounds were evaluated on trypomastigotes (Tulahuen β-gal strain, DTU-VI) that were co-incubated with Vero cells. Results revealed that lycorine (**104**), hippeastrine (**105**), haemanthamine (**107**), narciclasine (**108**), and montanine (**110**) were active. 1-O-acetylcaranine (**112**) could be considered weakly active (IC_{50} 35.59 μM), while the remaining compounds were inactive against the parasite (IC_{50} > 40 μM). The highest anti-*T. cruzi* activity rates were yielded by lycorine (**107**) (IC_{50} = 0.70 ± 0.02 μM) and narciclasine (**108**) (IC_{50} = 0.49 ± 0.02 μM), which exceeded in potency that of the reference drug BNZ (IC_{50} = 1.56 ± 0.07 μM). Haemanthamine (**107**) and montanine (**110**) showed average IC_{50} values similar to that of BNZ, 1.59 ± 0.06 μM and 1.99 ± 0.09 μM, respectively. Hippeastrine (**105**) was the active alkaloid with the highest IC_{50} value (3.63 ± 0.24 μM). Lycorine (**104**) and 1-O-acetylcaranine (**112**) belong to the lycorine sub-class of amaryllidaceae alkaloids, and structurally differ in two positions of the overall structure. In this case, the antiparasitic activity was increased by the substitution of a hydrogen and an acetoxy group per two hydroxyl groups. Toxicity against Vero and HepG2 cells was also evaluated. Lycorine (**104**) was found to be rather toxic on Vero cells (CC_{50} = 5.21 μM; SI:7.44) but moderately toxic for HepG2 with CC_{50} = 21.87 μM (SI: 31.24). Hippeastrine (**105**) did show low toxicity against Vero cells (CC_{50} = 45.99 ± 6.32 μM; SI:12.67) and HepG2 cells (CC_{50} = 128.1 ± 12.26 μM; SI: 35.29). Therefore, the anti-amastigote activity for this alkaloid was assessed (IC_{50} = 3.31 ± 0.39 μM), which was 2.75-fold higher than that of BZN (IC_{50} = 1.2 ± 0.22 μM) [53]. Crinine (**106**) was also isolated from fresh bulbs of *Crinum amabile*, another Amaryllidaceae, along with augustamine (**113**), augustine (**114**), augustine N-oxide (**115**), buphanisine (**116**), and buphanisine N-oxide (**117**) (Fig. 9). Extraction and fractionation of *Amaryllis belladonna* yielded 1-O-acetylcaranine (**112**), 3-O-acetylhamayne (**118**), and buphanamine (**119**) (Fig. 9). All of these compounds were tested against the

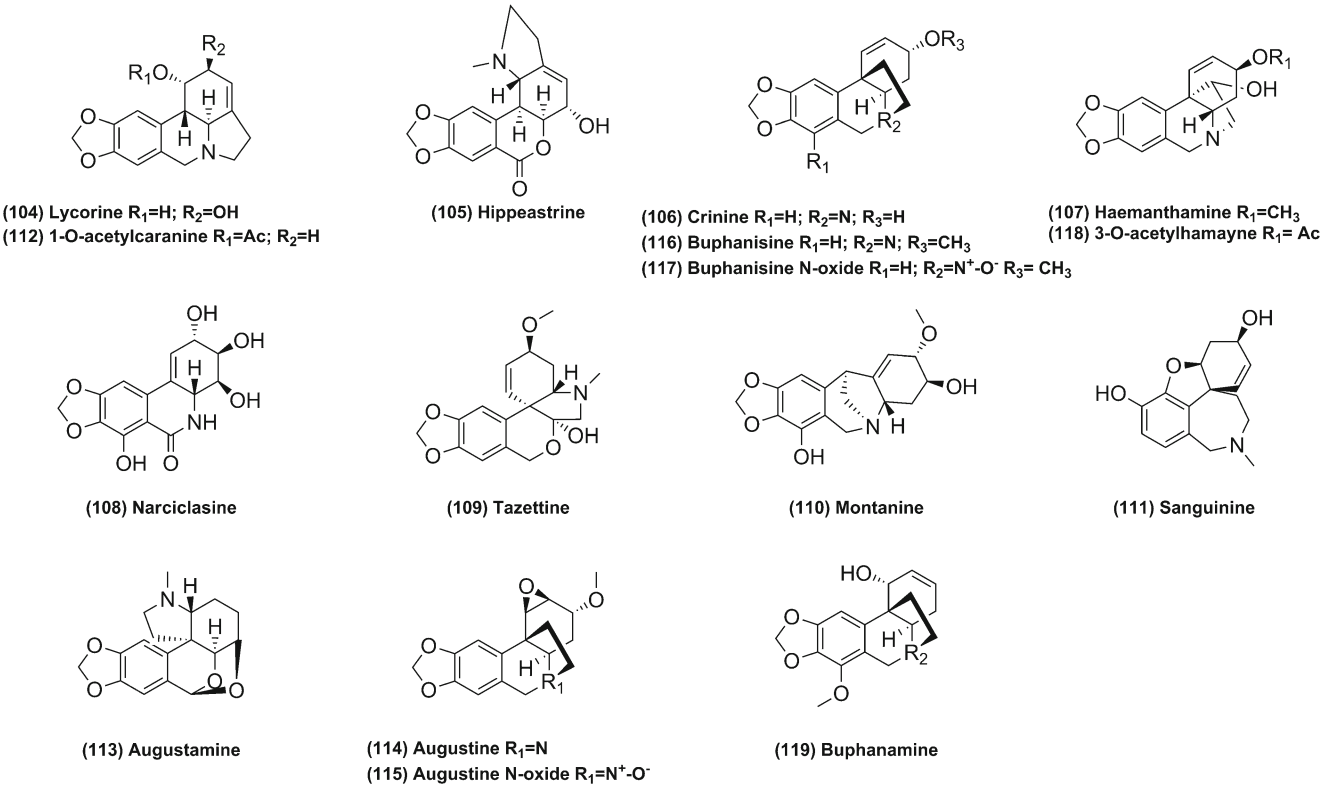

Fig. 9 Structures of compounds **104**–**119**

amastigote form (Tulahuen β-gal C2C4 strain). Compounds **106**, **112**–**117**, and **119** showed IC_{50} values higher than 100 μM while 3-O-acetylhamayne (**118**) presented moderate activity (IC_{50} 25.2 μM) and no cytotoxic effect on L6 cells [54, 55].

Guanidines

The guanidine-type alkaloids, batzelladine D (**120**), F (**121**), and L (**122**) and nor-batzelladine L (**123**) (Fig. 10A), were isolated from the marine sponge *Monanchora arbuscula.* Compounds were evaluated on free trypomastigotes (Y strain) and the IC_{50} values obtained were 64, 5, 2, and 7 μM, respectively. Cytotoxicity against LLC-MK2 cells was determined with CC_{50} values of 130, 10, 22, and 85 μM, respectively [56]. Compounds **122** and **123** had the highest SI (11 and 12, respectively). It appears that two tricyclic guanidine cores linked by an alkyl chain are more favorable than only one. Also, the length of the carbon chain at C-27 has some effect. Alchornedine (**124**) (Fig. 10A) was isolated from the leaves of *Alchornea glandulosa*. Trypomastigotes (Y strain) were susceptible to **124** and resulted in an IC_{50} value of 443 μM (95% confidence interval (CI) 388–505 μM) comparable to BZN (440 μM). Alchornedine (**124**) also showed activity against amastigotes, showing an IC_{50} value of 129 μM (95% CI: 81–205 μM), lower than BZN (IC_{50} value of 320 μM (95% CI: 286–357 μM). Despite the cytotoxicity of alchornedine (**124**) on mice conjunctive NCTC cells, which showed a CC_{50} value of 237 μM (95% CI: 189–298 μM), the compound displayed selectivity to intracellular forms. When amastigotes were hosted by mice peritoneal macrophages, the intracellular parasites were targeted without affecting the macrophages [57].

Other Alkaloids

Alternamide A (**125**) and B (**126**), and alternamine A (**127**) and B (**128**) (Fig. 11), presenting a catechol moiety which suggests a possible common biosynthetic route, were isolated from aerial parts of *Alternanthera littoralis* and evaluated against free trypomastigotes (Y strain). Except for alternamide B (**128**) which showed an IC_{50} value higher than 10 μM, the other compounds had IC_{50} values in the sub-micromolar range. The reported IC_{50} values for **125**, **127**, and **128** were 0.61 μM (95% CI: 0.55–0.82), 0.23 μM (95% CI: 0.20–0.26), and 0.82 μM (95% CI: 0.76–0.87) with crystal violet used as reference drug (IC_{50}: 0.18 μM). None of the compounds showed toxic effects against J774 macrophages in culture at concentrations up to 500 mg/mL [58].

Two terpenic indole alkaloids, polyalthenol (**129**) and N-acetyl-polyveoline (**130**) (Fig. 11), obtained from the root bark of *Greenwayodendron suaveolens* (Annonaceae) were evaluated against trypomastigotes (Tulahuen strain) resulting in an IC_{50} value of 8.4 μM for both of them (BZN IC_{50}: 2.13 μM), although cytotoxicity on MRC-5 cells showed a CC_{50} value of 5.8 and 29.8 μM, respectively [59].

Solamargine (**131**) (Fig. 11), a glycol-steroidal-alkaloid isolated from *Solanum palinacanthum*, was evaluated against epimastigotes of the Y strain and displayed moderate activity (IC_{50}: 17.63 μM, BZN IC_{50}: 34.58 μM) [60].

The sesquiterpene pyridine alkaloids, ilicifoliunines A (**132**) and B (**133**), aquifoliunine E-I (**134**), and mayteine (**135**) (Fig. 11), were isolated from the root bark of *Maytenus ilicifolia*. Compounds **133** and **135** showed no activity against the epimastigotes (Y strain) at 100 μM. Compounds **132** and **134** had an IC_{50} value of 27.7 and 41.9 μM and toxicity against murine macrophages showed a CC_{50} of 1282 μM (SI: 46.2) and 1847 μM (SI: 44.0), respectively [61].

Monalidine A (**136**) (Fig. 11), isolated from the marine sponge *Monanchora arbuscula*, showed an IC_{50} value of 8 μM against free trypomastigotes (Y strain) and a CC_{50} of 26 μM against LLC-MK2 cells [56].

Analogues and Semi-synthetic Modifications

With the strategy of combining the antiparasitic properties of natural *Cinchona* alkaloids with the known properties of bile acids as drug transporters, a series of 16 hybrids of *Cinchona* alkaloids and bile acids were prepared [62]. Eight out of 16 hybrids presented an IC_{50} around 1 μg/mL against trypomastigotes of the CL Brener strain (DTU-VI) and SI higher than 10 (**137**–**144**) (Fig. 12). Similar results were obtained when tested against trypomastigotes from the RA strain of *T. cruzi* (DTU-VI). The peracetylated and non-acetylated forms of the cinchonine/chenodeoxycholic bile acid conjugate (**139**–**140**) were the most trypanocidal hybrids against Y strain trypomastigotes, with IC_{50} values of 0.69 and 1.01 μM, respectively. Promising results were observed in invasion assays using the Y strain, where these hybrids induced a significant reduction in intracellular amastigotes and on the release of trypomastigotes from infected cells [62].

A series of 1-(substituted phenyl)-βcarbolines bearing an N-alkylcarboxamide (**145**–**156**) and methyl 6-oxobenzo[4,5]canthine-2-carboxylate derivatives (**157**–**162**) were synthetized and evaluated on Y strain epimastigotes (Fig. 7B and C) [63]. Some N-alkyl-1-(substituted phenyl)-β-carboline-3-carboxamides displayed high antitrypanosomal activity (IC_{50} = 3.22 ± 0.50–9.71 ± 1.70 μM) except for **148** and **156** that showed moderate activity (IC_{50} 14.20 ± 1.97 and 11.10 ± 1.77, respectively). However, the N-alkylcarboxamides series bearing the same alkyl groups were inactive against *T. cruzi* epimastigotes indicating better performance for molecules assembled on 1-(substituted

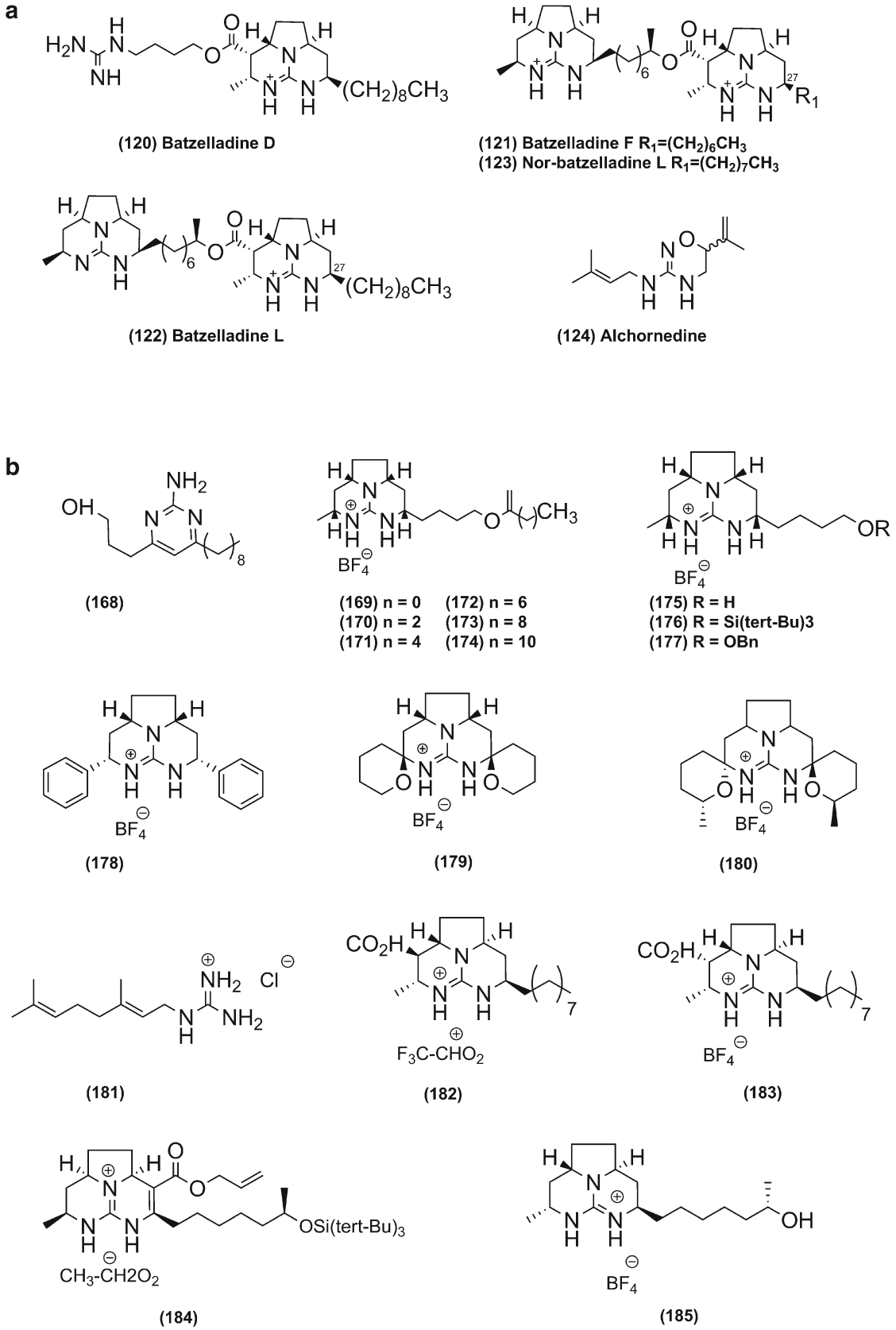

Fig. 10 Guanidines derived from the sponge *Monanchora arbuscula*. (A) Obtained from a natural source (**120**–**124**) or (B) obtained by synthesis (**168**–**185**)

phenyl)-β-carboline structure. The exception was N-alkylcarboxamides bearing N-methylpiperazylcarboxamide (**161**) and N-morpholylcarboxamide (**162**) groups at C-2 that showed high (IC_{50} = 0.40 ± 0.01 μM) or moderate (IC_{50} = 16.70 ± 1.27 μM) activity against *T. cruzi* parasites, respectively [63]. In addition, this study showed that the N-(substituted benzylidene)-carbohydrazide compounds (**163**–**167**) (Fig. 7D) were inactive. Since authors mentioned the antitumoral properties of β-carboline-type alkaloids, cell toxicity against several tumoral cell lines was also evaluated. The SI range of the most promising molecule (**161**) was 2.88–21.2 depending on the tissue-derived cell line used [63].

Eighteen guanidine-type alkaloids, analogues of the ones obtained from marine sponge *Monanchora arbuscula*, were synthesized (**168**–**185**) (Fig. 10B). Cytotoxicity was evaluated in NCTC cells and ranged between 2.4 μM and > 150 μM. The antitrypanosomal activity was tested against Y strain trypomastigotes (IC_{50} = 0.9–88.5 μM). The extension of the aliphatic chain and the substitution with the Si(*tert*-Bu)$_3$ of the analogues seems to be important since **168**, **172**–**174**, **176**, and **184** were the only active compounds. Coincidentally, these compounds showed low cytotoxicity with a SI greater than 10, except when BF_4 group was replaced by ethanoic acid that confers the most potent antiparasitic activity (IC_{50} = 0.9 μM), but high cytotoxicity as well (CC_{50} = 2 μM) [64].

Thirteen new semi-synthetic 1,2,4-triazole-3-thiones were obtained from natural piperine, the main constituent of the dried fruits of *Piper nigrum* (**186**–**198**) (Fig. 13). The variously substituted triazole derivatives were synthesized from the natural amide in four steps with overall yields ranging from 32 to 51%. The cyclohexyl substituted derivative (**191**) showed the best trypanocidal profile against the proliferative forms of T. cruzi (Y strain), with IC_{50} values of 18.3 and 8.87 μM against epimastigotes and amastigotes, respectively. No toxicity against peritoneal macrophages from Balb/c mice was observed [65].

Eighteen bromopyrrole alkaloids inspired in the natural pseudoceratidine (**199**) from the marine sponge *Tedania*

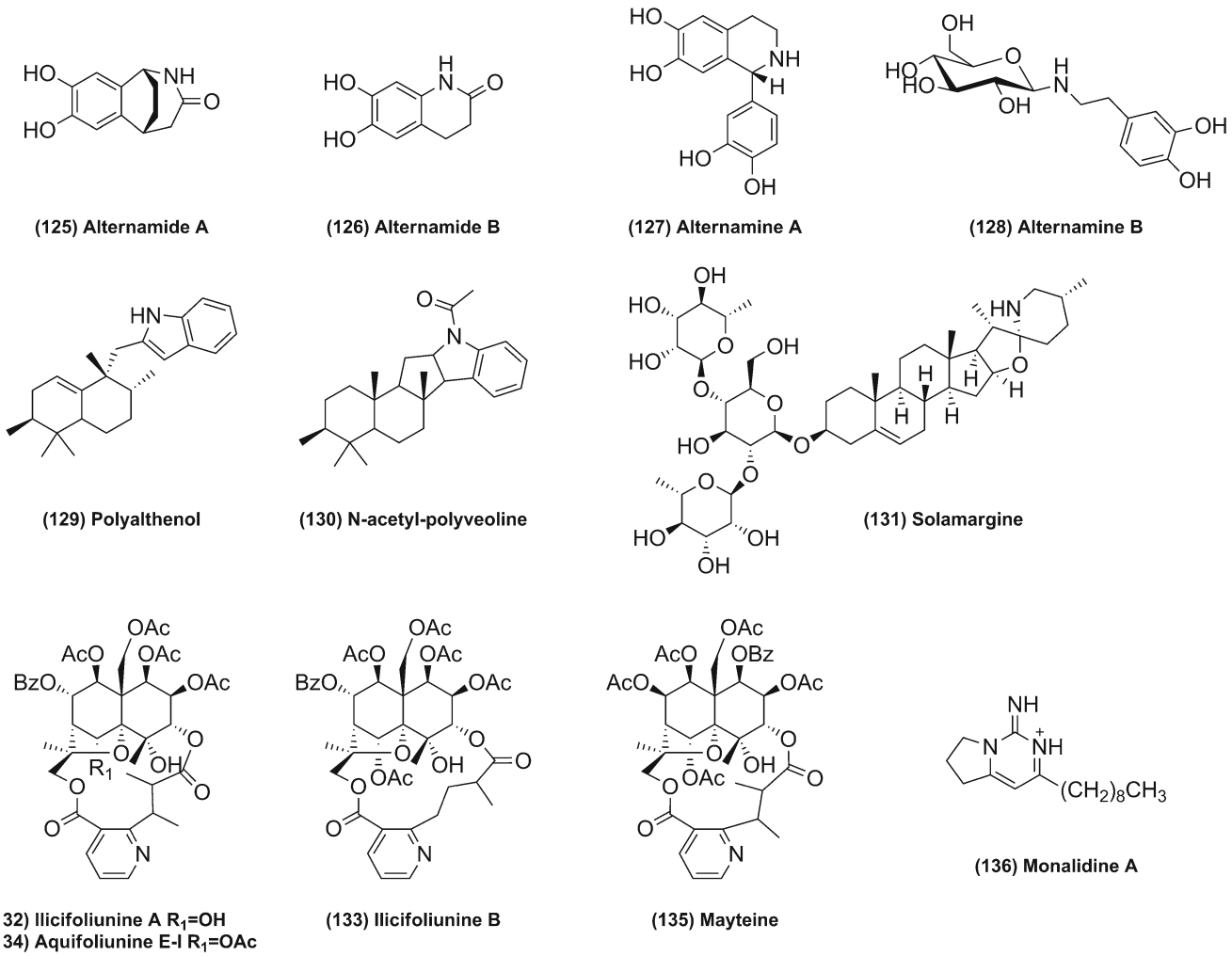

Fig. 11 Structure of compounds **125**–**136**

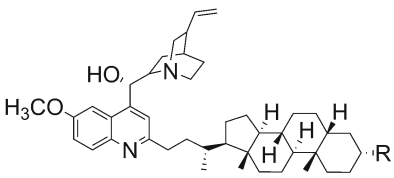

(137) Quinidine + Litocholic acid free R=OH
(138) Quinidine + Litocholic acid peracetylated R=OCH_3

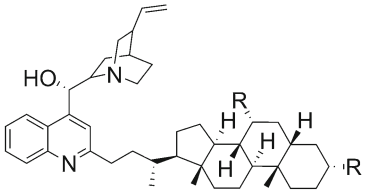

(139) Cinchonine + Chenodeoxycholic acid free R=OH
(140) Cinchonine + Chenodeoxycholic acid peracetylated R=OCH_3

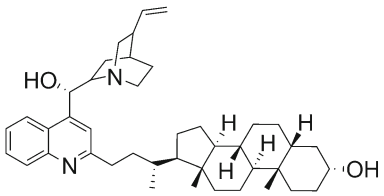

(141) Cinchonine + Litocholic acid free

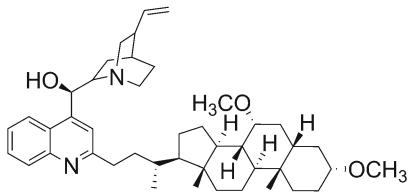

(142) Cinchonidine + Chenodeoxycholic peracetylated

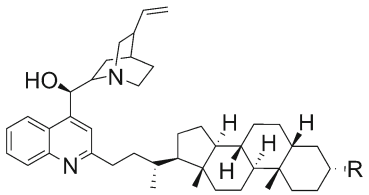

(143) Cinchonidine + Litocholic non-acetylated R=OH
(144) Cinchonidine + Litocholic peracetylated R=OCH_3

Fig. 12 Structure of compounds **137**–**144**

brasiliensis [66] were explored against epimastigotes *T. cruzi* (Y strain). Pseudoceratidine was synthetized (72% yield) in order to obtain enough amount for derivatization. Table 1 shows modifications regarding different alkyl chain length (**199** and **201**) or groups (**202**–**204**) in the linker between two pyrrole moieties. Compound **200** was the only compound of the series that showed activity against *T. cruzi* parasites (7.0 ± 1.0 μm) with a CC_{50} value of 52 ± 3 μM obtained against peritoneal murine macrophages. The introduction of a sulfur atom into the chain (**204**) displayed moderate trypanosomal activity (IC_{50} = 24 ± 4.0 μm). Additional variations were introduced into the pyrrole moiety and several derivatives were synthetized (**205**–**216**) (see Table 2); however, none of compounds displayed activity against *T. cruzi* parasites.

Fig. 13 Structure of compounds **186**–**198**

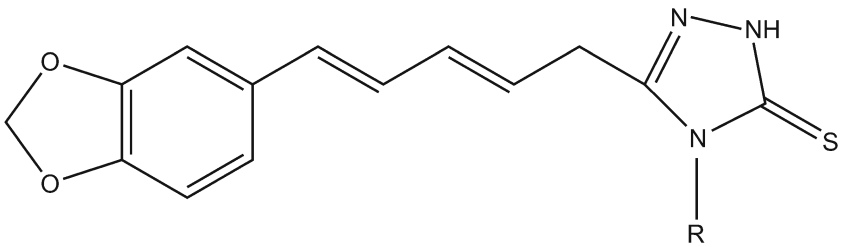

(186 - 198) 1,2,4-triazole-2-thiones

(186) R = Methyl
(187) R = Ethyl
(188) R = Isopropyl
(189) R = *n*-Butyl
(190) R = *n*- Hexyl
(191) R = Cyclohexyl
(192) R = Phenyl
(193) R = Benzyl
(194) R = 3,4,5-Trimethoxyphenyl
(195) R = tert-Butyl
(196) R = 4-(Methylthio)phenyl
(197) R = 3-Methoxyphenyl
(198) R = 4-(Trifluoromethyl)phenyl

Table 1 Structure of compounds **199–204**

Main structure		
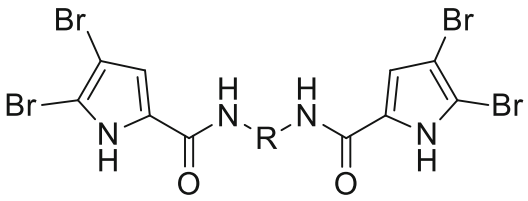		
Compound	**R**	
199	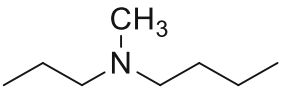	
200 -201	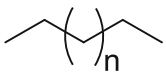	(200) n = 1 (201) n = 4
202	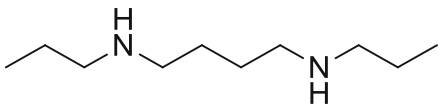	
203	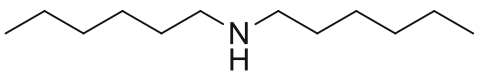	
204	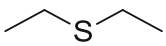	

Conclusion

Alkaloids are an interesting group of natural compounds with great structural diversity. Over the last 10 years, 132 natural alkaloids were evaluated against *T. cruzi*. Most of these (85.6%) were isolated from trees or plants, which is not surprising, considering that this material is more easily collected. Although microorganisms are great producers of these secondary metabolites, only two reports met the scope of this review. When analyzing the frequency of a specific type of structure, it was noticed that quinolines or isoquinolines represented more than 50% of the total, followed by indolic alkaloids (20.45%). Of the total, 39 structures (29.5%) showed IC_{50} below 10 μM against at least one parasite stage, and were considered active. Again, the activity appears to be bounded to quinolinic- or isoquinolic-type alkaloids. Mostly, sub-micromolar IC_{50} values were reported for quinolinones such as waltheriones and naphthylisoquinolines from *Ancistrocladus*. Among the active compounds, 13 substances (33.3%) displayed very good selectivity (SI > 30), at least for one cell line. Special attention is drawn to two compounds: 4′-O-demethylancistrocladinium A (**53**) and antidesmone (**71**),

Table 2 Structure of compounds **205**–**216**

Main structure		
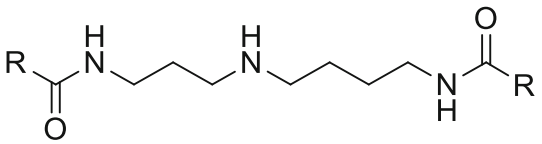		
Compound	**R**	**R1-R2**
205	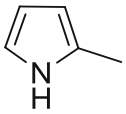	
206	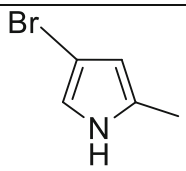	
207	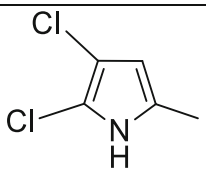	
208	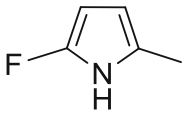	
209-210	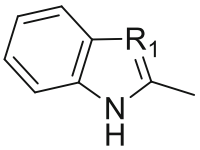	(**209**) R_1=CH (**210**) R_1=N
211-212	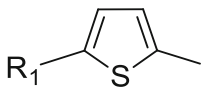	(**211**) R_1 = Br (**212**) R_1 = CH3
213-214	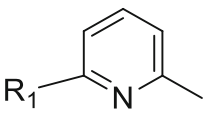	(**213**) R_1 = Br (**214**) R_1 = CH_3
215-216	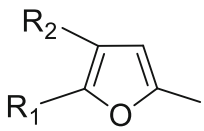	(**215**) R_1 = R_2 = Br (**216**) R_1 = CH_3; R_2 = H

both with IC_{50} values in the nanomolar range and CC_{50} values above 30 μM. These are good candidates to explore antiparasitic activity against all stages of different DTUs of *Trypanosoma cruzi* and its toxicity against an extended panel of cell lines. Among the 80 semi-synthetic molecules analyzed, cyclic structures whit N as heteroatom and bonded to quinolone ring might confer better performance against *T. cruzi* parasite forms. Moreover, alkaloids bearing cyclic

structures linked to a bile acid have increased membrane permeability (**139**–**140**) and showed potent activity against *T. cruzi* amastigote forms that guarantees further investigations. Novel and safer treatments for Chagas disease are needed and natural products will still play an important role in the development of a new generation of antichagasic drugs.

Funding Our research is supported by funding from the Agencia Nacional de Promoción Científica y Tecnológica, Argentina, PICT 2017-0425 to LRF and PICT 2015-1713 to MME.

Declarations

Conflict of Interest The authors declare no competing interests.

Human and Animal Rights and Informed Consent This article does not contain any studies with human or animal subjects performed by any of the authors.

References

Papers of particular interest, published recently, have been highlighted as:
- • Of importance
- •• Of major importance

1. de Moraes J, Geary TG. FDA-approved antiparasitic drugs in the 21st century: a success for helminthiasis? Trends Parasitol England. 2020;36:573–5.
2. Pollastri MP. Fexinidazole: a new drug for African sleeping sickness on the horizon. Trends Parasitol. 2018;34:178–9.
3. Deeks ED. Fexinidazole: first global approval. Drugs; New Zealand. 2019;79:215–20.
4. Morillo CA, Waskin H, Sosa-Estani S, del Carmen BM, Cuneo C, Milesi R, et al. Benznidazole and posaconazole in eliminating parasites in asymptomatic T. Cruzi Carriers: The STOP-CHAGAS Trial. J Am Coll Cardiol. 2017;69:939–47.
5.•• Urbina JA. Etiologic treatment of Chagas Disease: old drugs, new insights, challenges, and perspectives. Chagas Dis. Springer International Publishing; 2020. p. 123–44. **This work extensively describes the state of the art of the most recent clinical trials against Chagas Disease and its outcomes and provides very interesting insights.**
6. Achan J, Talisuna AO, Erhart A, Yeka A, Tibenderana JK, Baliraine FN, et al. Quinine, an old anti-malarial drug in a modern world: role in the treatment of malaria. Malar J. 2011;10:144.
7. Berman JD. Approval of tafenoquine for malaria chemoprophylaxis. Am J Trop Med Hyg. 2019;100:1301–4.
8. Monteón VM, Furuzawa-Carballeda J, Alejandre-Aguilar R, Aranda-Fraustro A, Rosales-Encina JL, Reyes PA. American trypanosomosis: in situ and generalized features of parasitism and inflammation kinetics in a murine model. Exp Parasitol. Academic Press Inc. 1996;83:267–74.
9. Zingales B, Andrade SG, Briones MRS, Campbell DA, Chiari E, Fernandes O, et al. A new consensus for Trypanosoma cruzi intraspecific nomenclature: second revision meeting recommends TcI to TcVI. Mem Inst. Oswaldo Cruz. Fundacao Oswaldo Cruz. 2009;104:1051–4.
10. Moreno M, D'ávila DA, Silva MN, Galvão LM, MacEdo AM, Chiari E, et al. Trypanosoma cruzi benznidazole susceptibility in vitro does not predict the therapeutic outcome of human Chagas disease. Mem Inst. Oswaldo Cruz Fundacao Oswaldo Cruz. 2010;105:918–24.
11. Villarreal D, Barnabé C, Sereno D, Tibayrenc M. Lack of correlation between in vitro susceptibility to Benznidazole and phylogenetic diversity of Trypanosoma cruzi, the agent of Chagas disease. Exp Parasitol. 2004;108:24–31.
12. Filardi LS, Brener Z. Susceptibility and natural resistance of Trypanosoma cruzi strains to drugs used clinically in Chagas disease. Trans R Soc Trop Med Hyg. 1987;81:755–9.
13. Barbosa H, da Silva RLCG, Costa-Silva TA, Tempone AG, Antar GM, Lago JHG, et al. Interaction of dicentrinone, an antitrypanosomal aporphine alkaloid isolated from Ocotea puberula (Lauraceae), in cell membrane models at the air-water interface. Bioorg Chem Elsevier. 2020;101:103978.
14. da Silva DB, Tulli ECO, Militão GCG, Costa-Lotufo LV, Pessoa C, de Moraes MO, et al. The antitumoral, trypanocidal and antileishmanial activities of extract and alkaloids isolated from Duguetia furfuracea. Phytomedicine. 2009;16:1059–63.
15. Costa EV, Pinheiro MLB, De Souza ADL, Barison A, Campos FR, Valdez RH, et al. Trypanocidal activity of oxoaporphine and pyrimidine-β-carboline alkaloids from the branches of annona foetida mart. (annonaceae). Molecules. 2011;16:9714–20.
16. Ibrahim SRM, Mohamed GA. Naphthylisoquinoline alkaloids potential drug leads. Fitoterapia. Elsevier B.V.; 2015. p. 194–225.
17. Bringmann G, Hamm A, Günther C, Michel M, Brun R, Mudogo V. Ancistroealaines A and B, two new bioactive naphthylisoquinolines, and related naphthoic acids from Ancistrocladus ealaensis. J Nat Prod. 2000;63:1465–70.
18. Bringmann G, Spuziak J, Faber JH, Gulder T, Kajahn I, Dreyer M, et al. Six naphthylisoquinoline alkaloids and a related benzopyranone from a Congolese Ancistrocladus species related to Ancistrocladus congolensis. Phytochemistry. 2008;69:1065–75.
19. Bringmann G, Saeb W, Rückert M, Mies J, Michel M, Mudogo V, et al. Ancistrolikokine D, a 5,8′-coupled naphthylisoquinoline alkaloid, and related natural products from Ancistrocladus likoko. Phytochemistry. 2003;62:631–6.
20. Bringmann G, Messer K, Brun R, Mudogo V. Ancistrocongolines A-D, new naphthylisoquinoline alkaloids from Ancistrocladus congolensis. J Nat Prod. 2002;65:1096–101.
21. Mufusama JP, Feineis D, Mudogo V, Kaiser M, Brun R, Bringmann G. Antiprotozoal dimeric naphthylisoquinolines, mbandakamines B3 and B4, and related 5,8′-coupled monomeric alkaloids, ikelacongolines A-D, from a Congolese: Ancistrocladus liana. RSC Adv R Soc Chem. 2019;9:12034–46.
22. Bringmann G, Dreyer M, Faber JH, Dalsgaard PW, Stærk D, Jaroszewski JW, et al. Ancistrotanzanine A, the first 5,3'-coupled naphthylisoquinoline alkaloid, and two further, 5,8′-linked related compounds from the newly described species Ancistrocladus tanzaniensis. J Nat Prod. 2003;66:1159–65.
23. Bringmann G, Seupel R, Feineis D, Zhang G, Xu M, Wu J, et al. Ancistectorine D, a naphthylisoquinoline alkaloid with antiprotozoal and antileukemic activities, and further 5,8'- and 7,1'-linked metabolites from the Chinese liana Ancistrocladus tectorius. Fitoterapia. Elsevier B.V. 2016;115:1–8.
24. Lombe BK, Feineis D, Mudogo V, Brun R, Awale S, Bringmann G. Michellamines A6 and A7, and further mono- and dimeric naphthylisoquinoline alkaloids from a Congolese: Ancistrocladus liana and their antiausterity activities against pancreatic cancer cells. RSC Adv. 2018;8:5243–54.
25. Fayez S, Feineis D, Aké Assi L, Kaiser M, Brun R, Awale S, et al. Ancistrobrevines E-J and related naphthylisoquinoline alkaloids from the West African liana Ancistrocladus abbreviatus with

inhibitory activities against Plasmodium falciparum and PANC-1 human pancreatic cancer cells. Fitoterapia. Elsevier. 2018;131:245–59.
26. Bringmann G, Dreyer M, Faber JH, Dalsgaard PW, Jaroszewski JW, Ndangalasi H, et al. Ancistrotanzanine C and related 5,1‘- and 7,3‘-coupled naphthylisoquinoline alkaloids from Ancistrocladus tanzaniensis. J Nat Prod Am Chem Soc. 2004;67:743–8.
27. Bringmann G, Dreyer M, Rischer H, Wolf K, Hadi HA, Brun R, et al. Ancistrobenomine A, the first naphthylisoquinoline oxygenated at Me-3, and related 5,1′-coupled alkaloids, from the “new” plant species Ancistrocladus benomensis. J Nat Prod. 2004;67:2058–62.
28. Bringmann G, Seupel R, Feineis D, Xu M, Zhang G, Kaiser M, et al. Antileukemic ancistrobenomine B and related 5,1′-coupled naphthylisoquinoline alkaloids from the Chinese liana Ancistrocladus tectorius. Fitoterapia. 2017;121:76–85.
29. Bringmann G, Messer K, Wolf K, Mühlbacher J, Grüne M, Brun R, et al. Dioncophylline E from Dioncophyllum thollonii, the first 7,3′-coupled dioncophyllaceous naphthylisoquinoline alkaloid. Phytochemistry. 2002;60:389–97.
30. Bringmann G, Dreyer M, Michel M, Tayman FSK, Brun R. Ancistroheynine B and two further 7,3′-coupled naphthylisoquinoline alkaloids from Ancistrocladus heyneanus Wall. Phytochemistry. 2004;65:2903–7.
31. Bringmann G, Wohlfarth M, Rischer H, Schlauer J, Brun R. Extract screening by HPLC coupled to MS–MS, NMR, and CD: a dimeric and three monomeric naphthylisoquinoline alkaloids from Ancistrocladus griffithii. Phytochemistry. 2002;61:195–204.
32. Bringmann G, Messer K, Schwöbel B, Brun R, Aké AL. Habropetaline a, an antimalarial naphthylisoquinoline alkaloid from triphyophyllum peltatum. Phytochemistry. 2003;62:345–9.
33. Bringmann G, Dreyer M, Kopff H, Rischer H, Wohlfarth M, Hadi HA, et al. ent-dioncophylleine A and related dehydrogenated naphthylisoquinoline alkaloids, the first Asian dioncophyllaceae-type alkaloids, from the “new” plant species Ancistrocladus benomensis. J Nat Prod. 2005;68:686–90.
34. Bringmann G, Kajahn I, Reichert M, Pedersen SEH, Faber JH, Gulder T, et al. Ancistrocladinium A and B, the first N,C-coupled naphthyldihydroisoquinoline alkaloids, from a Congolese Ancistrocladus species. J Org Chem Am Chem Soc. 2006;71:9348–56.
35. Bringmann G, Zhang G, Büttner T, Bauckmann G, Kupfer T, Braunschweig H, et al. Jozimine A2: The first dimeric dioncophyllaceae-type naphthylisoquinoline alkaloid, with three chiral axes and high antiplasmodial activity. Chem - A Eur J. 2013;19:916–23.
36. Li J, Seupel R, Bruhn T, Feineis D, Kaiser M, Brun R, et al. Jozilebomines A and B, Naphthylisoquinoline dimers from the Congolese Liana Ancistrocladus ileboensis, with antiausterity activities against the PANC-1 human pancreatic cancer cell line. J Nat Prod. 2017;80:2807–17.
37. Tshitenge DT, Bruhn T, Feineis D, Mudogo V, Kaiser M, Brun R, et al. An unusually broad series of seven cyclombandakamines, bridged dimeric naphthylisoquinoline alkaloids from the Congolese Liana Ancistrocladus ealaensis. Sci Rep. 2019;9:1–12.
38. Tshitenge DT, Feineis D, Mudogo V, Kaiser M, Brun R, Bringmann G. Antiplasmodial ealapasamines A-C,’mixed’ naphthylisoquinoline dimers from the Central African Liana Ancistrocladus ealaensis. Sci Rep. 2017;7:1–9.
39. Costa RS, Souza Filho OP, Júnior OCSD, Silva JJ, Le Hyaric M, Santos MAV, et al. In vitro antileishmanial and antitrypanosomal activity of compounds isolated from the roots of Zanthoxylum tingoassuiba. Rev Bras. Sociedade Brasileira de Farmacognosia. 2018;28:551–8.
40. Biavatti MW, Vieira PC, Da Silva MFDGF, Fernandes JB, Victor SR, Pagnoccab FC, et al. Biological activity of quinoline alkaloids from Raulinoa echinata and X-ray structure of flindersiamine. J Braz Chem Soc. 2002;13:66–70.
41. Mwangi ESK, Keriko JM, Machocho AK, Wanyonyi AW, Malebo HM, Chhabra SC, et al. Antiprotozoal activity and cytotoxicity of metabolites from leaves of Teclea trichocarpa. J Med Plant Res. 2010;4:726–31.
42. Cretton S, Breant L, Pourrez L, Ambuehl C, Marcourt L, Ebrahimi SN, et al. Antitrypanosomal quinoline alkaloids from the roots of waltheria indica. J Nat Prod. 2014;77:2304–11.
43. Cretton S, Bréant L, Pourrez L, Ambuehl C, Perozzo R, Marcourt L, et al. Chemical constituents from Waltheria indica exert in vitro activity against Trypanosoma brucei and T. cruzi. Fitoterapia. Elsevier B.V. 2015;105:55–60.
44. Bringmann G, Schlauer S, Rischer H, Wohlfahrt M, Haller R, Bär S, et al. Antidesmone, a novel antitrypanosomal alkaloid. Pharm Pharmacol Lett. 2001;11:47–8.
45. Braga M V, De Souza W. E¡ects of protein kinase and phosphatidylinositol-3 kinase inhibitors on growth and ultrastructure of Trypanosoma cruzi. 2006
46. Assefa D, Worku Y, Skoglund G. Protein kinase activities in Leishmania aethiopica: control by growth, transformation and inhibitors. Biochim Biophys Acta Netherlands. 1995;1270:157–62.
47. Cartuche L, Sifaoui I, López-Arencibia A, Bethencourt-Estrella CJ, Nicolás-Hernández DS, Lorenzo-Morales J, et al. Antikinetoplastid activity of indolocarbazoles from streptomyces sanyensis. Biomolecules. 2020;10:1–14.
48. Ferreira ME, Cebrián-Torrejón G, Corrales AS, Vera De Bilbao N, Rolón M, Gomez CV, et al. Zanthoxylum chiloperone leaves extract: first sustainable Chagas disease treatment. J Ethnopharmacol Elsevier Ireland Ltd. 2011;133:986–93.
49.• Bilsland E, Tavella TA, Krogh R, Stokes JE, Roberts A, Ajioka J, et al. Antiplasmodial and trypanocidal activity of violacein and deoxyviolacein produced from synthetic operons. BMC Biotechnol. 2018;18:1–8 **This work provides an original approach to the obtaintion of natural products in a more sustainable way.**
50. Martínez-Luis S, Gómez JF, Spadafora C, Guzmán HM, Gutiérrez M. Antitrypanosomal alkaloids from the marine bacterium Bacillus pumilus. Molecules. 2012;17:11146–55.
51. Reina M, Ruiz-Mesia W, Ruiz-Mesia L, Martínez-Díaz R, González-Coloma A. Indole alkaloids from Aspidosperma rigidum and A. schultesii and their antiparasitic effects. Zeitschrift fur Naturforsch - Sect C. J Biosci. 2011;66(C):225–34.
52. Reina M, Ruiz-Mesia W, López-Rodríguez M, Ruiz-Mesia L, González-Coloma A, Martínez-Díaz R. Indole alkaloids from Geissospermum reticulatum. J Nat Prod. 2012;75:928–34.
53. Martinez-Peinado N, Cortes-Serra N, Torras-Claveria L, Pinazo MJ, Gascon J, Bastida J, et al. Amaryllidaceae alkaloids with anti-Trypanosoma cruzi activity. Parasites and Vectors. BioMed Central. 2020;13:1–10.
54. Tallini LR, de Andrade JP, Kaiser M, Viladomat F, Nair JJ, Zuanazzi JAS, et al. Alkaloid constituents of the amaryllidaceae plant amaryllis belladonna L. Molecules. 2017;22.
55. Tallini LR, Torras-Claveria L, de Souza BW, Kaiser M, Viladomat F, Zuanazzi JAS, et al. N-oxide alkaloids from crinum amabile (amaryllidaceae). Molecules. 2018;23:1–11.
56. Santos MFC, Harper PM, Williams DE, Mesquita JT, Pinto ÉG, Da Costa-Silva TA, et al. Anti-parasitic Guanidine and Pyrimidine Alkaloids from the Marine Sponge Monanchora arbuscula. J Nat Prod. 2015;78:1101–12.
57. Barrosa KH, Pinto EG, Tempone AG, Martins EGA, Lago JHG. Alchornedine, a new anti - Trypanosomal guanidine alkaloid from Alchornea glandulosa. Planta Med. 2014;80:1310–4.

58. Koolen HHF, Pral EMF, Alfieri SC, Marinho JVN, Serain AF, Hernández-Tasco AJ, et al. Antiprotozoal and antioxidant alkaloids from Alternanthera littoralis. Phytochemistry. 2017;134:106–13.
59. Muganza DM, Fruth B, Nzunzu JL, Tuenter E, Foubert K, Cos P, et al. In vitro antiprotozoal activity and cytotoxicity of extracts and isolated constituents from Greenwayodendron suaveolens. J Ethnopharmacol Elsevier. 2016;193:510–6.
60. Moreira RRD, Martins GZ, Magalhães NO, Almeida AE, Pietro RCLR, Silva FAJ, et al. In vitro trypanocidal activity of solamargine and extracts from Solanum palinacanthum and Solanum lycocarpum of brazilian cerrado. An Acad Bras Cienc. 2013;85:903–7.
61. Santos VAFFM, Regasini LO, Nogueira CR, Passerini GD, Martinez I, Bolzani VS, et al. Antiprotozoal sesquiterpene pyridine alkaloids from Maytenus ilicifolia. J Nat Prod. 2012;75:991–5.
62. Musikant D, Leverrier A, Bernal D, Ferri G, Palermo JA, Edreira MM. Hybrids of cinchona alkaloids and bile acids as antiparasitic agents against Trypanosoma cruzi. Molecules. 2019;24:1–9.
63. Silva CMBL, Garcia FP, Da Silva Rodrigues JH, Nakamura CV, Ueda-Nakamura T, Meyer E, et al. Synthesis, antitumor, antitrypanosomal and antileishmanial activities of benzo[4, 5]canthin-6-ones bearing the N′-(substituted benzylidene)-carbohydrazide and N-alkylcarboxamide groups at C-2. Chem Pharm Bull. 2012;60:1372–9.
64. Martins LF, Mesquita JT, Pinto EG, Costa-Silva TA, Borborema SET, Galisteo Junior AJ, et al. Analogues of marine guanidine alkaloids are in vitro effective against Trypanosoma cruzi and selectively eliminate Leishmania (L.) infantum intracellular amastigotes. J Nat Prod. 2016;79:2202–10.
65. Franklim TN, Freire-De-Lima L, De Nazareth Sá Diniz J, Previato JO, Castro RN, Mendonça-Previato L, et al. Design, synthesis and trypanocidal evaluation of novel 1,2,4-triazoles-3- thiones derived from natural piperine. Molecules. 2013;18:6366–82.
66. Parra LLL, Bertonha AF, Severo IRM, Aguiar ACC, De Souza GE, Oliva G, et al. Isolation, derivative synthesis, and structure-activity relationships of antiparasitic bromopyrrole alkaloids from the Marine Sponge Tedania brasiliensis. J Nat Prod. 2018;81:188–202.